Top-quark pair production in heavy-ion collisions with the ATLAS experiment

Patrycja Potępa[1,2,*] on behalf of the ATLAS Collaboration

[1]AGH University of Krakow, al. Adama Mickiewicza 30, 30-059 Kraków, Poland
[2]Johannes Gutenberg University Mainz, Saarstr. 21, 55122 Mainz, Germany

Abstract. Measurements of top quarks in heavy-ion collisions are expected to provide novel probes of nuclear modifications to parton distribution functions as well as to bring unique information about the evolution of strongly interacting matter. We report the observation of the top-quark pair production in proton-lead collisions at the centre-of-mass energy of 8.16 TeV in the ATLAS experiment at the LHC. Top-quark pair production is measured in the lepton+jets and the dilepton channels, with a significance well above 5 standard deviations in each channel separately. The results from the measurement of the nuclear modification factor $R_{p\mathrm{A}}$ are also presented.

ATL-PHYS-PROC-2025-015
26 February 2025

1 Introduction

Ultra-relativistic heavy-ion collisions at the Large Hadron Collider (LHC) provide a unique opportunity to study nuclear modifications to parton distribution functions (nPDF) [1]. A wide acceptance of the ATLAS detector [2] offers a possibility to measure several types of probes, including top quarks. As the heaviest elementary particles carrying colour charges, top quarks are considered to be attractive probes of nPDFs in the high Bjorken-x region of $3\cdot10^{-3}-0.5$, which is difficult to access using other available probes. Since top-quark pair ($t\bar{t}$) production is dominated by gluon–gluon fusion, the $t\bar{t}$ process is sensitive to the gluon nPDF, which is particularly important for perturbative calculations in Quantum Chromodynamics.

With the large luminosities of proton–lead (p+Pb) data collected during Run 2, top-quark yields become experimentally accessible. The analysed data were collected in 2016 with the ATLAS detector, yielding a total integrated luminosity of of 165 nb^{-1}. Data taking was conducted in two configurations: p+Pb and Pb+p beam directions, corresponding to integrated luminosities of 57 and 108 nb^{-1}, respectively. The proton and lead-ion beams had an energy of 6.5 TeV and 2.56 TeV per nucleon, respectively, resulting in a nucleon–nucleon centre-of-mass collision energy of $\sqrt{s_{\mathrm{NN}}} = 8.16$ TeV and a rapidity boost by +0.465 units in the p-going direction relative to the laboratory frame. The $t\bar{t}$ process is studied in the combined ℓ+jets and dilepton channel, involving electrons and muons in the final state [3].

*e-mail: patrycja.potepa@cern.ch

2 Event selection

Top-quark pairs are reconstructed using final states with electrons and muons. The events are selected using single-electron and single-muon triggers with a minimum transverse momentum (p_{T}) threshold of 15 GeV [4]. At least one reconstructed vertex, built from at least two good-quality charged-particle tracks with $p_{\mathrm{T}} > 0.1$ GeV is required. Reconstructed electron (muon) candidates are required to have $p_{\mathrm{T}} > 18$ GeV and $|\eta| < 2.47$ (2.5), and satisfy 'Medium' identification and isolation criteria [5, 6]. Jets are built using the anti-k_t algorithm [7] with a radius parameter $R = 0.4$. Jets originating from b-quarks (b-jets) are tagged using the DL1r algorithm [8]. A fake-lepton background contribution is estimated from data using the Matrix Method technique [9].

Events with exactly one lepton and at least four jets form the ℓ+jets channel, while events with exactly two opposite-sign leptons and at least two jets constitute the dilepton channel. The ℓ+jets channel is divided into four signal regions with one electron or muon and exactly one or at least two b-jets, labelled as $1\ell 1b$ e+jets, $1\ell 2b$incl e+jets, $1\ell 1b$ μ+jets, and $1\ell 2b$incl μ+jets. Another two signal regions are defined in the dilepton channel, characterized by exactly one or at least two b-jets, labelled as $2\ell 1b$ and $2\ell 2b$incl, respectively. Figure 1 shows distributions of $H_{\mathrm{T}}^{\ell j}$ in the six signal regions, where $H_{\mathrm{T}}^{\ell j}$ is the scalar sum of the transverse momenta of leptons and jets.

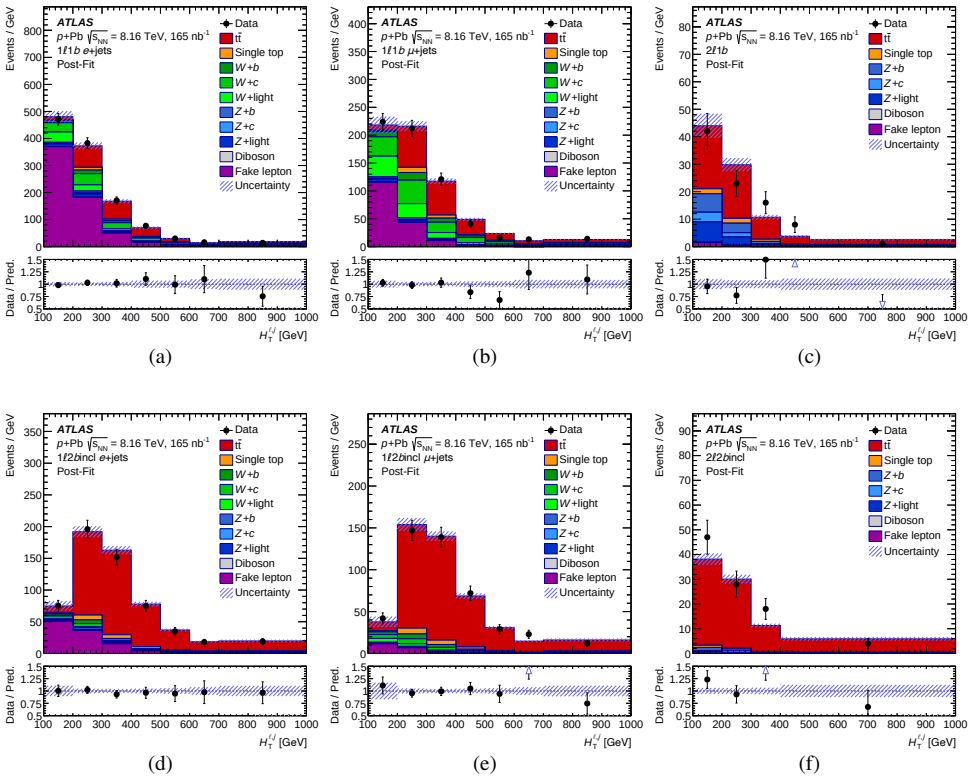

Figure 1: Comparison of data and total post-fit prediction for the $H_{\mathrm{T}}^{\ell,j}$ distribution in each of the six signal regions (e+jets: (a) $1\ell 1b$ and (d) $1\ell 2b$incl, μ+jets: (b) $1\ell 1b$ and (e) $1\ell 2b$incl, dilepton: (c) $2\ell 1b$ and (f) $2\ell 2b$incl), with uncertainties represented by the hatched area [3].

3 Analysis strategy

A profile-likelihood method [10] is used to extract the signal strength $\mu_{t\bar{t}}$, which is defined as the ratio of the observed $t\bar{t}$ cross-section in the combined ℓ+jets and dilepton channels to the Standard Model (SM) expectation with no nPDF effects involved. The value of $\mu_{t\bar{t}}$ is determined by the simultaneous fit to the $H_{\mathrm{T}}^{\ell,j}$ distributions in data in the six signal regions.

Systematic uncertainties affecting the measurement originate from electron, muon, and jet reconstruction, b-tagging performance, fake-lepton background estimation, the signal and background modelling, and integrated luminosity. The dominant sources of systematic uncertainty arise from the jet energy scale and the modelling of the $t\bar{t}$ process. The total relative systematic uncertainty in $\mu_{t\bar{t}}$ amounts to 8%.

Figure 2 presents the best-fit values of $\mu_{t\bar{t}}$ extracted from the individual signal regions and in the combined fit. $\mu_{t\bar{t}}$ values in all signal regions are consistent with each other and the SM prediction ($\mu_{t\bar{t}} = 1$) within the total uncertainties. The total uncertainty is primarily driven by the systematic component in the ℓ+jets channel and the statistical component in the dilepton channel. The background-only hypothesis is rejected with a significance above five standard deviations separately in ℓ+jets and dilepton decay modes, resulting in the first observation of the $t\bar{t}$ process in the dilepton channel in p+Pb collisions.

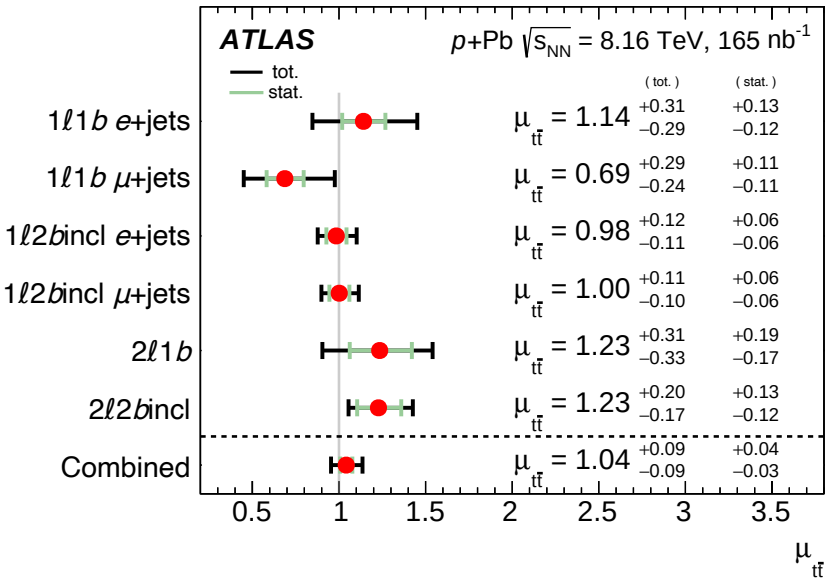

Figure 2: Observed best-fit values of the signal strength with statistical and systematic uncertainties in each signal region and in the combined fit [3].

4 Results

The observed value of $\mu_{t\bar{t}}$ is translated into the $t\bar{t}$ production cross-section in p+Pb collisions using the following formula

$$\sigma_{t\bar{t}}^{p+\mathrm{Pb}} = \mu_{t\bar{t}} \cdot A_{\mathrm{Pb}} \cdot \sigma_{t\bar{t}}^{\mathrm{th}}, \tag{1}$$

where $A_{\mathrm{Pb}} = 208$ stands for the lead mass number and $\sigma_{t\bar{t}}^{\mathrm{th}}$ is the theoretical $t\bar{t}$ cross-section in nucleon–nucleon collisions computed at the NNLO precision in QCD. The inclusive $t\bar{t}$ cross-section in p+Pb collisions is measured to be

$$\sigma_{t\bar{t}}^{p+\mathrm{Pb}} = 58.1 \pm 2.0\ (\mathrm{stat.})\ ^{+4.8}_{-4.4}\ (\mathrm{syst.})\ \mathrm{nb} = 58.1\ ^{+5.2}_{-4.9}\ (\mathrm{tot.})\ \mathrm{nb}. \tag{2}$$

The total relative uncertainty is 9%, leading to the most precise $t\bar{t}$ cross-section measurement in heavy-ion collisions.

The obtained $t\bar{t}$ cross-section is contrasted with the theoretical predictions and other experimental results in Figure 3. The result is in agreement with predictions based on four state-of-the-art nPDF sets: TUJU21 [11], nNNPDF3.0 [12], nCTEQ15HQ [13], and EPPS21 [14]. The measurement is consistent with the $t\bar{t}$ cross-section reported by CMS [15] within the total uncertainties. The result is also in agreement with the combined $t\bar{t}$ cross-section in pp collisions at $\sqrt{s} = 8$ TeV by ATLAS and CMS [16], scaled to the p+Pb system by A_{Pb} and extrapolated to the centre-of-mass energy of this measurement.

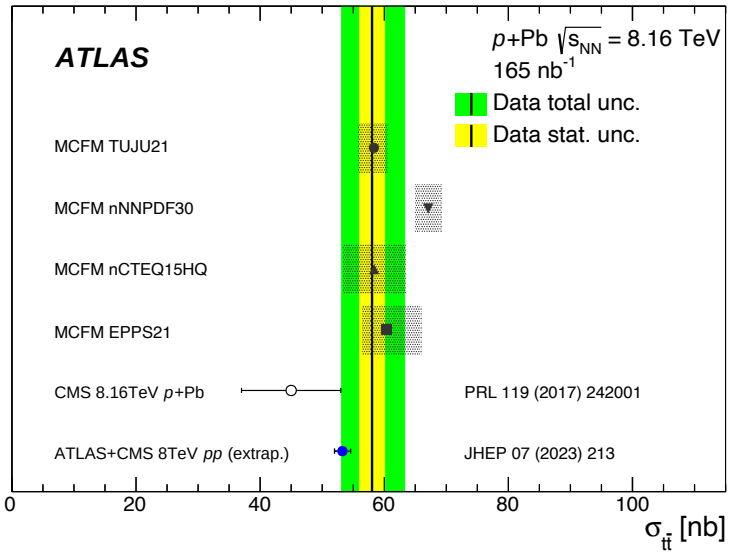

Figure 3: Comparison of the $t\bar{t}$ cross-section with theoretical predictions and other measurements [3].

Differences between p+Pb and pp systems are quantified using the nuclear modification factor, $R_{p\mathrm{A}}$, expressed by the following formula

$$R_{p\mathrm{A}} = \frac{\sigma_{t\bar{t}}^{p+\mathrm{Pb}}}{A_{\mathrm{Pb}} \cdot \sigma_{t\bar{t}}^{pp}}, \tag{3}$$

where $\sigma_{t\bar{t}}^{pp}$ denotes the observed $t\bar{t}$ cross-section in pp collisions [16], extrapolated to centre-of-mass energy of this measurement. All uncertainties in the cross-section measurements in p+Pb and pp collisions are treated as uncorrelated. The obtained $R_{p\mathrm{A}}$ value amounts to

$$R_{p\mathrm{A}} = 1.090 \pm 0.039\ (\mathrm{stat.})\ ^{+0.094}_{-0.087}\ (\mathrm{syst.}) = 1.090 \pm 0.100\ (\mathrm{tot.}) \tag{4}$$

The measured $R_{p\mathrm{A}}$ is consistent with the geometric expectation from the pp system within one standard deviation. Figure 4 shows a comparison of the observed $R_{p\mathrm{A}}$ value with predictions based on the four nPDF sets. The uncertainty related to the baseline PDF for pp interactions is assumed to be fully correlated between predictions in the pp and p+Pb systems, and cancels out in the ratio. The result is in agreement with the theoretical predictions, with the largest difference of more than one standard deviation for the nNNPDF3.0 nPDF set.

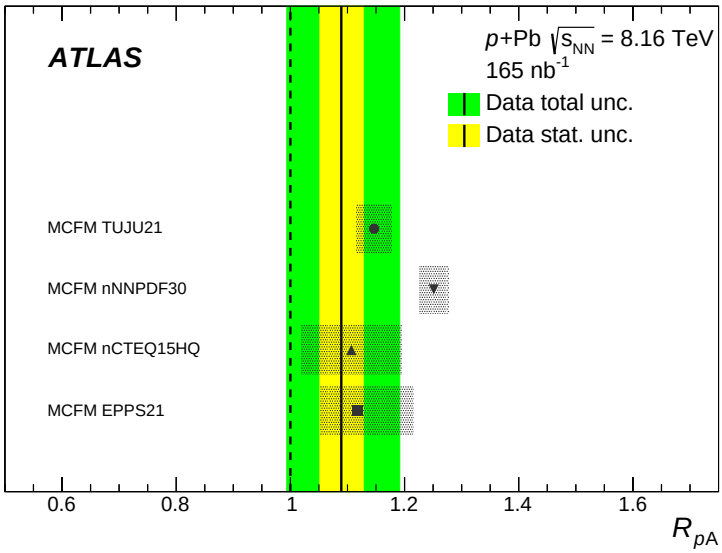

Figure 4: Comparison of the nuclear modification factor for $t\bar{t}$ production with theoretical predictions and other measurements [3].

5 Conclusions

The measurement is focused on $t\bar{t}$ production in p+Pb collisions at $\sqrt{s_{\mathrm{NN}}}$ = 8.16 TeV in the ATLAS experiment. The inclusive $t\bar{t}$ cross-section is extracted with the total relative uncertainty of 9%, leading to the most precise $t\bar{t}$ cross-section result in heavy-ion collisions to date. The nuclear modification factor for the $t\bar{t}$ process is also extracted for the first time. The results are found to be consistent with theoretical predictions based on four state-of-the-art nPDF sets.

With the precision of this measurement, it provides a valuable input to constraining nPDFs in the high Bjorken-x region. It also paves the way for future measurements of $t\bar{t}$ production in heavy-ion collisions, including studies of quark-gluon plasma properties in Pb+Pb collisions at the LHC.

Acknowledgements

This work was partly supported by the National Science Centre of Poland under grant UMO-2020/37/B/ST2/01043, by program „Excellence initiative – research university" project no 9722 for the AGH University of Krakow, and by PL-Grid Infrastructure.

References

[1] K.J. Eskola, P. Paakkinen, H. Paukkunen, C.A. Salgado, EPPS21: a global QCD analysis of nuclear PDFs, Eur. Phys. J. C **82**, 413 (2022), 2112.12462. 10.1140/epjc/s10052-022-10359-0

[2] ATLAS Collaboration, The ATLAS Experiment at the CERN Large Hadron Collider, Journal of Instrumentation **3**, S08003 (2008). 10.1088/1748-0221/3/08/S08003

[3] ATLAS Collaboration, Observation of $t\bar{t}$ production in the lepton+jets and dilepton channels in p+Pb collisions at $\sqrt{s_{\mathrm{NN}}}$ = 8.16 TeV with the ATLAS detector, JHEP **11**, 101 (2024), [arXiv]2405.05078. 10.1007/JHEP11(2024)101

[4] ATLAS Collaboration, Performance of the ATLAS Trigger System in 2015, Eur. Phys. J. C **77**, 317 (2017), 1611.09661. 10.1140/epjc/s10052-017-4852-3

[5] ATLAS Collaboration, Electron and photon performance measurements with the ATLAS detector using the 2015–2017 LHC proton-proton collision data, Journal of Instrumentation **14**, P12006 (2019). 10.1088/1748-0221/14/12/p12006

[6] ATLAS Collaboration, Muon reconstruction and identification efficiency in ATLAS using the full Run 2 pp collision data set at $\sqrt{s}$ = 13 TeV, Eur. Phys. J. C **81**, 578 (2021), [arXiv]2012.00578. 10.1140/epjc/s10052-021-09233-2

[7] M. Cacciari, G.P. Salam, G. Soyez, The anti-k_t jet clustering algorithm, JHEP **04**, 063 (2008), 0802.1189. 10.1088/1126-6708/2008/04/063

[8] ATLAS Collaboration, ATLAS b-jet identification performance and efficiency measurement with $t\bar{t}$ events in pp collisions at $\sqrt{s}$ = 13 TeV, Eur. Phys. J. C **79**, 970 (2019), 1907.05120. 10.1140/epjc/s10052-019-7450-8

[9] ATLAS Collaboration, Tools for estimating fake/non-prompt lepton backgrounds with the ATLAS detector at the LHC, JINST **18**, T11004 (2023), 2211.16178. 10.1088/1748-0221/18/11/T11004

[10] K. Cranmer, G. Lewis, L. Moneta, A. Shibata, W. Verkerke, HistFactory: A tool for creating statistical models for use with RooFit and RooStats, CERN-OPEN-2012-016, New York (2012), https://cds.cern.ch/record/1456844

[11] I. Helenius, M. Walt, W. Vogelsang, TUJU21: nuclear PDFs with electroweak-boson data at NNLO, in *29th International Workshop on Deep-Inelastic Scattering and Related Subjects* (2022), [arXiv]2207.04654

[12] R. Abdul Khalek, R. Gauld, T. Giani, E.R. Nocera, T.R. Rabemananjara, J. Rojo, nNNPDF3.0: evidence for a modified partonic structure in heavy nuclei, Eur. Phys. J. C **82**, 507 (2022), [arXiv]2201.12363. 10.1140/epjc/s10052-022-10417-7

[13] P. Duwentäster, T. Ježo, M. Klasen, K. Kovařík, A. Kusina, K.F. Muzakka, F.I. Olness, R. Ruiz, I. Schienbein, J.Y. Yu, Impact of heavy quark and quarkonium data on nuclear gluon PDFs, Phys. Rev. D **105**, 114043 (2022), [arXiv]2204.09982. 10.1103/PhysRevD.105.114043

[14] K.J. Eskola, P. Paakkinen, H. Paukkunen, C.A. Salgado, EPPS21: a global QCD analysis of nuclear PDFs, Eur. Phys. J. C **82**, 413 (2022), [arXiv]2112.12462. 10.1140/epjc/s10052-022-10359-0

[15] CMS Collaboration, Observation of top quark production in proton-nucleus collisions, Phys. Rev. Lett. **119**, 242001 (2017), [arXiv]1709.07411. 10.1103/PhysRevLett.119.242001

[16] ATLAS and CMS Collaborations, Combination of inclusive top-quark pair production cross-section measurements using ATLAS and CMS data at $\sqrt{s}$ = 7 and 8 TeV, JHEP **07**, 213 (2023), [arXiv]2205.13830. 10.1007/JHEP07(2023)213